Continental Shelf Research, Vol. 4, No. 6, pp. 661 to 680, 1985.
Printed in Great Britain.

0278–4343/85 £3.00 + 0.00

Satellite observations of phytoplankton variability during an upwelling event

MARK R. ABBOTT*† and PHILIP M. ZION†

(*Received* 20 *August* 1984; *in revised form* 26 *November* 1984; *accepted* 28 *November* 1984)

Abstract—A sequence of satellite images of near-surface phytoplankton pigment concentrations and sea surface temperature together with concurrent surface measurements are used to study an upwelling event during the Coastal Ocean Dynamics Experiment off northern California. These data sets show a high degree of temporal and spatial variability during this episode. Recurrent patterns in this variability give insight into the dynamics of coastal upwelling and its effects on biological distributions. Simple models of coastal upwelling cannot explain the observed phenomena in the CODE region. Satellite estimates of phytoplankton growth rates were about 0.8 day^{-1} near persistent upwelling centers.

INTRODUCTION

THE study of upwelling systems has received much attention recently, focusing on both the biological and physical processes within such systems (BOJE and TOMCZAK, 1978; RICHARDS, 1981). We present results obtained from satellite observations of near-surface phytoplankton pigment concentrations and sea surface temperature during a single upwelling event in early July 1981 off northern California. These observations, associated with concurrent ship, buoy, and drifter measurements, provide a high resolution temporal and spatial view of upwelling that would be impossible to obtain using only a single data source.

The Coastal Ocean Dynamics Experiment (CODE) was conducted during spring and summer of 1981 and 1982. The intent of CODE was to identify and study the key processes governing the wind-driven circulation over the continental shelf (CODE GROUP, 1983). Two small-scale arrays were deployed that were heavily instrumented with meteorological and oceanographic equipment. In addition, regular ship CTD surveys were conducted along with drifter releases and aircraft surveys. [See CODE GROUP (1983) for a description of the data sets and preliminary results.]

The use of Coastal Zone Color Scanner (CZCS) and Advanced Very High Resolution Radiometer (AVHRR) imagery in the study of coastal ecosystems has been increasing. [A description of the CZCS can be found in HOVIS (1981); a description of the AVHRR can be found in SCHWALB (1978).] During CODE, KELLY (1983) analyzed AVHRR imagery to describe the relationship of sea surface temperature (SST) to wind forcing and topography. This study showed the importance of local wind events in creating the observed patterns of SST. We present results from a study of CZCS imagery also collected during CODE. By

* Scripps Institution of Oceanography, A–002, University of California, La Jolla, CA 92093, U.S.A.
† Jet Propulsion Laboratory, California Institute of Technology, 4800 Oak Grove Drive, Pasadena, CA 91109, U.S.A.

comparing CZCS and AVHRR imagery, we attempt to characterize the temporal and spatial evolution of the phytoplankton pigment distribution during an upwelling event. We also explore the relationship of these distributions to physical forcing processes.

Comparisons between SST and chlorophyll have been made during several cruises to various upwelling regions (BEERS *et al.*, 1971; BRINK *et al.*, 1981; JONES *et al.*, 1983). In general, these results show that SST tracks the 'age' of a particular parcel of upwelled water. Thus, the coldest water is the most recently upwelled and has a low chlorophyll content. Warmer water has a higher chlorophyll content, which reaches a maximum value and then decreases with increasing temperature. However, problems of synopticity and spatial variability hamper the determination of the origin of a particular water parcel. Satellite imagery may prove useful in describing such upwelling systems, where mesoscale variability is intense.

METHODS

AVHRR and CZCS imagery was collected at the Scripps Satellite Oceanography Facility. Copies of the raw data were processed at the Jet Propulsion Laboratory using software provided by O. Brown and R. Evans (Rosenstiel School of Marine and Atmospheric Science University of Miami) as installed on the JPL Pilot Ocean Data System. The raw data were first corrected for geographic errors resulting from inaccuracies in time, roll, pitch, and yaw, as well as in the tilt angle for the moveable mirror on the CZCS. It has been estimated that a particular pixel can be located to within 3 km (GORDON *et al.*, 1983a) using this software system. After correction, a 1024-by-1024 pixel array was removed from each satellite pass, using 39°N, 125°W as the center point.

Geophysical algorithms were then applied to derive SST and near-surface pigment concentrations. SST was estimated using the channel 4 (10 to 11.5 μm) brightness temperature. Although more sophisticated algorithms exist (MCCLAIN *et al.*, 1983; BERNSTEIN, 1982), we use simple channel 4 temperatures. Although this method will produce SST images with relatively large mean temperature differences (KELLY, 1983), we are concerned more with relative spatial patterns, rather than absolute temperature values. Near-surface pigment was derived using algorithms described by GORDON *et al.* (1983a, b). [See also ZION (1983) for a description of CZCS processing.] We assume a marine aerosol type for all of the images (R. EVANS, personal communication). Pigment values should be accurate to about ± 0.3 log ⟨pigment⟩. Examination of mean pigment values in this time series showed fluctuations to be well within this range.

These images of SST and pigment were then resampled and remapped to an equal area, 512-by-512 grid. The remapped arrays were also centered at 39°N, 125°W with a spatial resolution of 1 km^2. The final arrays are directly comparable over time and between sensors as corresponding pixels cover the same geographic location. Photographs of the SST and pigment images from CODE-1 can be found in KELLY (1982) and ABBOTT and ZION (1984).

Surface measurements made during early July 1981 consisted of a CTD survey (OLIVERA, 1982; OLIVERA *et al.*, 1982), surface drifter releases (DAVIS, 1983, 1985a, b), and continuous moored and shore-based current and meteorological measurements (ROSENFELD, 1983). The CTD survey took place between 4 and 14 July from Pt. Arena to Purisima Point (Fig. 1; Purisima Point is at 34.75°N, 120.67°W). Drifter releases were made on 4, 9, and 14 July at Pt. Arena. The drifters were tracked by aircraft for several days after release (DAVIS, 1985a).

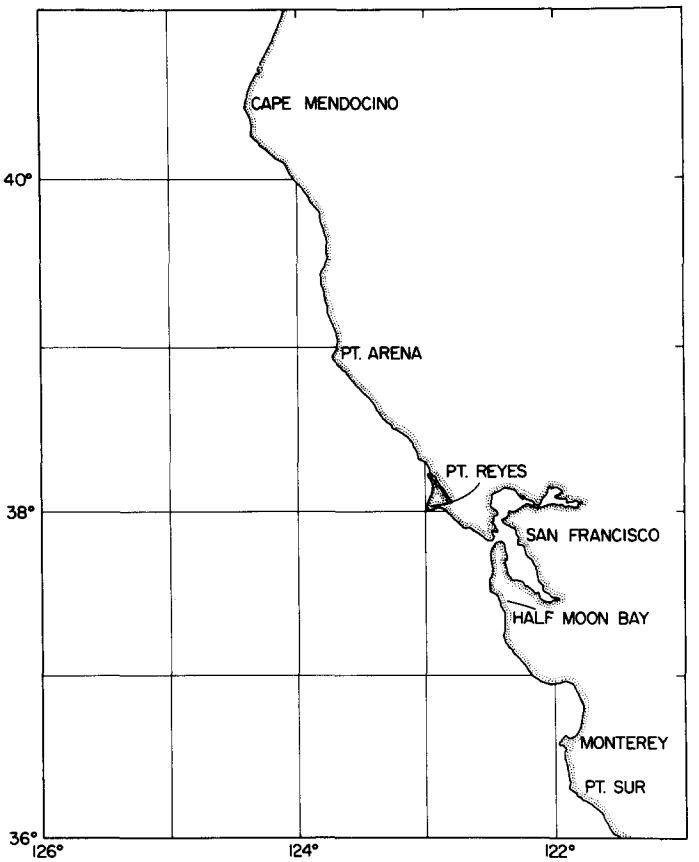

Fig. 1. Map of northern California coast.

RESULTS

The CODE area is in the region of the highest summer wind stress along the west coast of North America (NELSON, 1977; HICKEY, 1979). During late June 1981, a low pressure system occupied much of the area and was associated with considerable cloudiness. This period was followed by a strong high pressure system in the Pacific northwest resulting in strong southward winds. Figure 2 shows the low-passed wind stress vectors from the C3 meteorological buoy located at 38.61°N, 123.47°W during a 12-day period in early July with strong, upwelling-favorable winds. Such conditions resulted in relatively less cloud cover as well, creating excellent satellite viewing conditions.

Analysis of the CTD survey revealed three water mass types: cold, saline, freshly upwelled water near the coast; warm, fresh water offshore (thought to be a remnant of the Columbia River plume); and warm, saline water near the coast south of San Francisco (OLIVERA, 1982). Large-scale currents were nearly geostrophic and meandering. The highest velocities were observed within the frontal areas between the freshly upwelled saline water and fresh, warm offshore water.

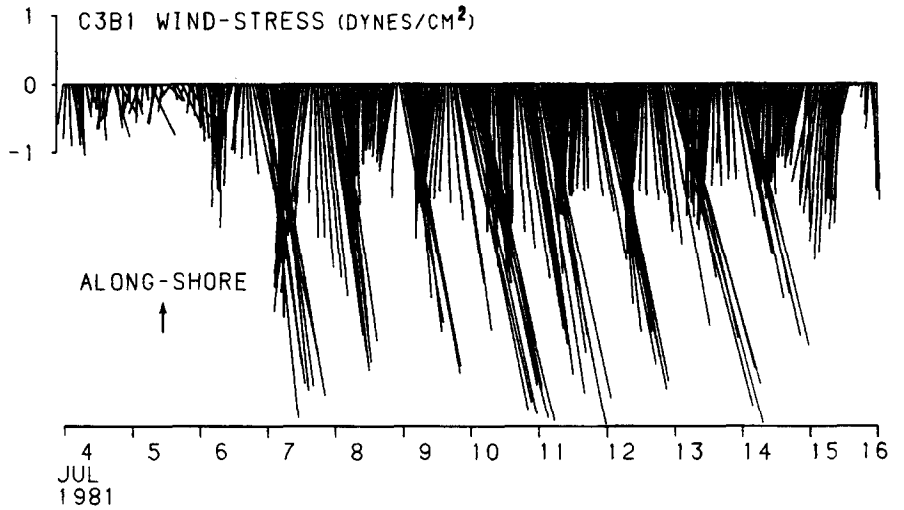

Fig. 2. Wind stress time series at C3 mooring during period of 4 to 15 July 1981. The wind stress vectors are plotted with the alongshore component (directed towards 317°T) oriented up in the figure. Note the diurnal modulation in the alongshelf component associated with the local sea-breeze. Figure courtesy of R. C. Beardsley.

Drifter tracks showed complicated patterns of near-surface currents with preferred areas of offshore transport (DAVIS, 1985a, b). Velocities in these regions were often in excess of 50 cm s^{-1}. Eddy processes appeared to be particularly important in the flow dynamics (DAVIS, 1985b). Empirical orthogonal function analysis of the entire CODE-1 AVHRR imagery data set showed early July to be a period of strong upwelling with well-developed jets located at Cape Mendocino and Pt. Arena (KELLY, 1983).

Figures 3 and 4 show two pairs of AVHRR and CZCS images from 8 and 14 July 1981. There was considerable mesoscale variability which was dominated by a series of eddies and meanders. Such features in the temperature field are associated with features in the velocity field (KELLY, 1983; CODE GROUP, 1983). These patterns are surface manifestations of features that encompass at least the mixed layer (KELLY, 1983; DAVIS, 1985a; MOOERS and ROBINSON, 1984; RIENECKER *et al.*, 1985) and are not confined to a thin surface layer. On 8 July (Fig. 3, top), there was a distinct southern boundary to the nearshore zone of upwelled, cold water at Pt. Reyes. Examination of data beyond the southern limit of the image (Monterey) showed generally warmer water near the coast as far as Pt. Conception. This warm water appears to be the warm, saline water mass described by OLIVERA (1982), related to the observed decrease in wind stress south of Pt. Reyes (KELLY, 1983). There were large meanders leaving the coast at Cape Mendocino and Pt. Reyes, associated with strong offshore flow (OLIVERA, 1982). These meanders are related to variations in the coastline topography and the spatial patterns of wind relaxation (KELLY, 1983). Similar features have been described by BERNSTEIN *et al.* (1977), BREAKER and GILLIAND (1981), MOOERS and ROBINSON (1984), and RIENECKER *et al.* (1985). Within the nearshore upwelling band, there were isolated regions adjacent to the coast that were cooler than the surrounding area, in particular near Cape Mendocino and Pt. Arena. Such features have been noted in other upwelling systems (BRINK *et al.*, 1981; JONES *et al.*, 1983) and are typically associated with features in the coastline (MILLOT and WALD, 1981).

The 14 July SST image (Fig. 3, bottom) was collected as the southward winds began to relax, and there was a shoreward advance of the offshore cloud bank. The nearshore cold water now had a northern boundary near Cape Mendocino. The southern boundary had moved north past Pt. Reyes. Such northward movement of warm water during wind relaxations may create surface convergences in the vicinity of Pt. Reyes (DAVIS, 1985a).

The pigment images from 8 and 14 July (Fig. 4) were acquired approximately 3 h before the SST images. The two sets were similar at large scales. For example, the large plume off Pt. Arena in the 8 July image (Fig. 4, top) had a similar structure in SST. Some features were more apparent in the pigment image, such as the cold core eddy (KELLY, 1983; DAVIS, 1985a) off Pt. Arena which had very high pigment concentrations. The area of lower pigment nearshore between Pt. Arena and Pt. Reyes was associated with the region of slightly lower nearshore temperatures. There were other features that had no apparent analog in SST. For example, a nearshore area of low pigment north of Pt. Arena had no corollary in SST. By 14 July (Fig. 4, bottom), the low pigment area south of Pt. Arena had increased in size and decreased in mean concentration. The low pigment area north of Pt. Arena behaved similarly, but it propagated northward (intervening images confirmed this movement; the net propagation speed was about 2 cm s^{-1}). Finally, there were two regions of persistently high pigment north of Cape Mendocino and south of Pt. Reyes.

SST and phytoplankton pigment are two non-conservative tracers. SST can change as a result of heating and cooling; pigment can change as a result of phytoplankton growth, death, and sinking. However, SST is not a passive scalar as it clearly affects the dynamics of the flow. Although pigment concentrations affect light absorption and hence heating of the upper layers (LEWIS *et al.*, 1983), pigment is more nearly a passive scalar. Because of the nonlinear coupling between the physical and biological dynamics (DENMAN, 1983), we expect SST and pigment to behave differently. Recent theoretical work by BENNETT and DENMAN (1985) discusses the behavior of a passive, non-conservative scalar in two-dimensional turbulence.

One way to compare the two variables is by plotting the joint frequency distribution of observed pigment concentration and SST. Such comparisons have been made in many upwelling systems (BEERS *et al.*, 1971; BRINK *et al.*, 1981; JONES *et al.*, 1983). Figure 5 shows such a plot comparing the satellite-derived pigment values and the ship-measured SST (OLIVERA *et al.*, 1982). (Comparisons between pigment and salinity and pigment and σ_T were nearly identical.) As the ship CTD survey took 9 days, we used the CZCS image closest in time to each station. Despite the mismatch in sampling times, Fig. 5 has the same general shape derived from other upwelling areas. That is, pigment is low at low SST, increases at higher SST, reaches a maximum value, and then decreases at the highest SST's. Such a relationship is consistent with the following scenario. Cold, nutrient-rich, but low pigment concentration water is upwelled to the surface and then advected away from this upwelling center. As this water is exposed to high solar radiation, phytoplankton grow rapidly and SST increases. Eventually, nutrients are exhausted, and pigment concentrations decrease while SST continues to increase. Warm, offshore water not directly influenced by upwelling will also have low pigment concentrations.

Variability in such relationships based on ship observations may be aliased by the long time required for ship sampling, particularly in a highly energetic region. Figure 6 shows six pigment–temperature surfaces derived from the six pairs of CZCS–AVHRR images acquired during this upwelling event. As there were more than 90,000 usable points (neither cloud nor land) for each pair (200,000 for the clear scenes from 7 and 8 July), we have color-coded each pigment–temperature locus by the number of occurrences. (Some residual cloud effects

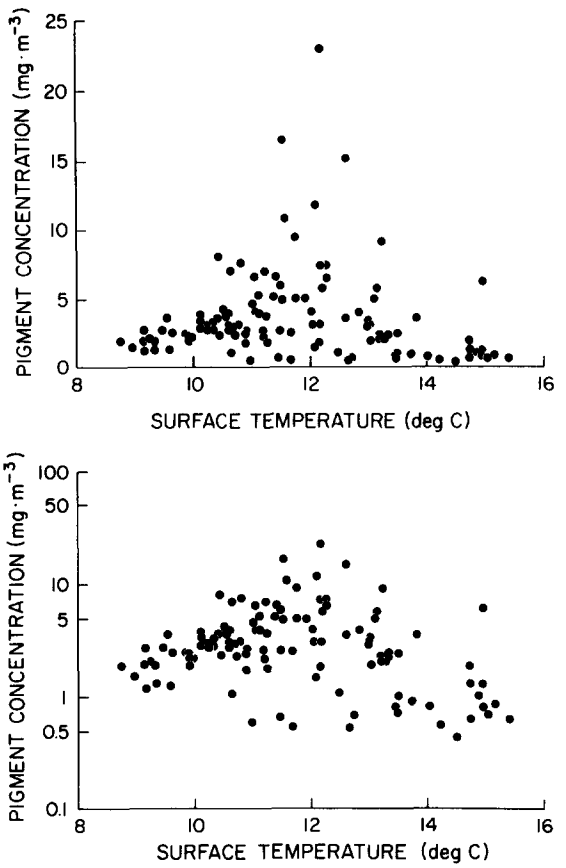

Fig. 5. Scatter plot of ship-measured SST and satellite-estimated phytoplankton pigment concentration. Upper panel has arithmetic axis for pigment while lower panel has logarithmic axis for pigment.

remain in the CZCS images as a result of incomplete masking, particularly in areas of sensor saturation near very bright clouds.) The correlation coefficient between log ⟨pigment⟩ and SST is also shown in the figure caption. The vertical striping is a result of missing temperature values caused by the digitization of the satellite signals. Although there was time separation between the pigment and SST images (about 8 h for pairs with NOAA-6 images and about 3 h for pairs with NOAA-7 images), movement of features should be relatively small between images (about 15 km for an 8-h separation and velocities of 50 cm s^{-1}).

These surfaces showed some of the expected relationships between SST and pigment concentration. The 6 July image (Fig. 6a) showed a nearly log-linear decrease in pigment with increasing SST. A similar relationship was present in the 7 July image (Fig. 6b). (The reduced scatter in Fig. 6b was a result of less cloud contamination on 7 July.) By 8 July (Fig. 6c) this surface had become more complex, with the appearance of low SST, low pigment water. Although there was some cloud contamination on 9 July (Fig. 6d), the shape of the surface resembled that of 8 July. By 13 and 14 July (Fig. 6e and f) the complexity of the pigment–SST surface had increased further. Low pigment, low SST water was more apparent. However, there was also more water with high pigment, high SST, a relationship that was relatively uncommon on 8 July (Fig. 6c).

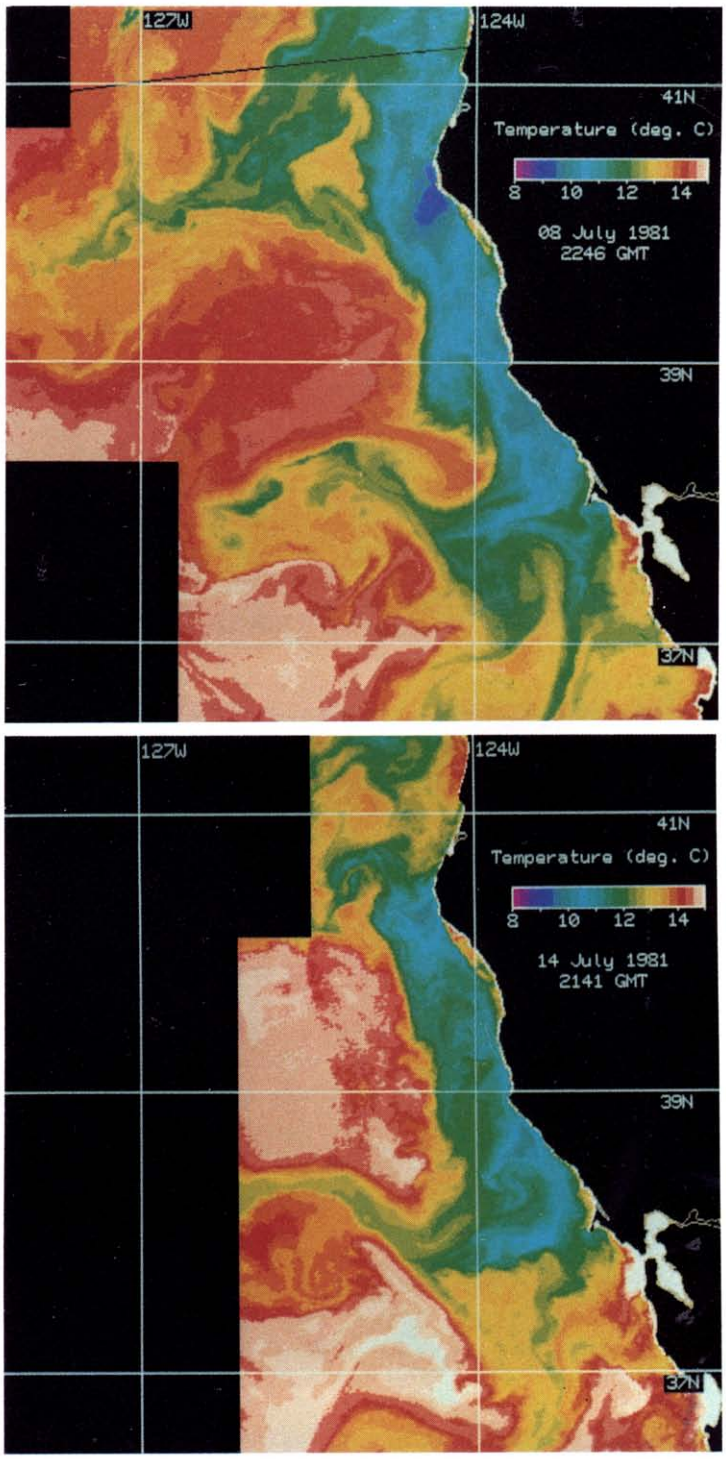

Fig. 3. AVHRR (from NOAA-7) images from 8 and 14 July 1981. Clouds and land have beer masked. Images are approximately 560 km on a side.

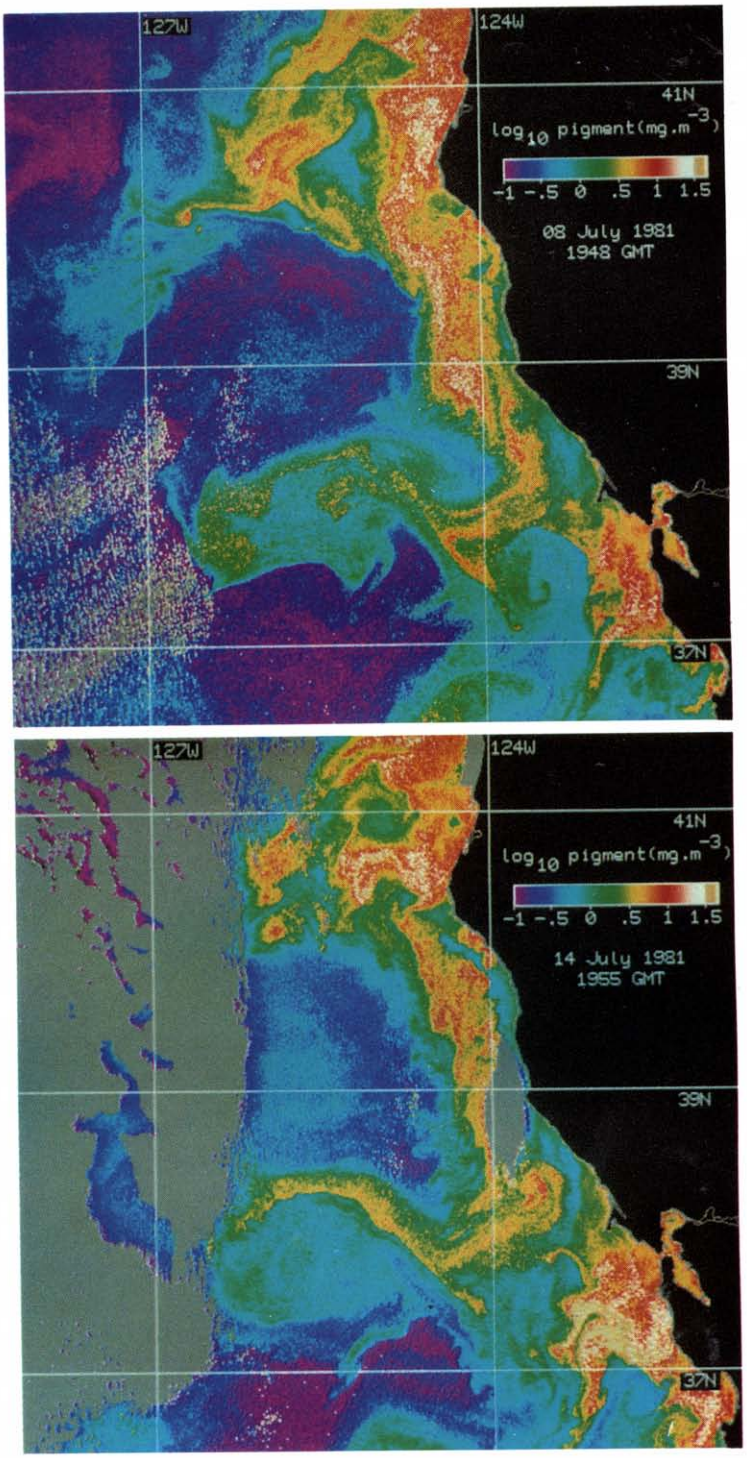

Fig. 4. CZCS images from 8 and 14 July 1981. Clouds and land have been masked

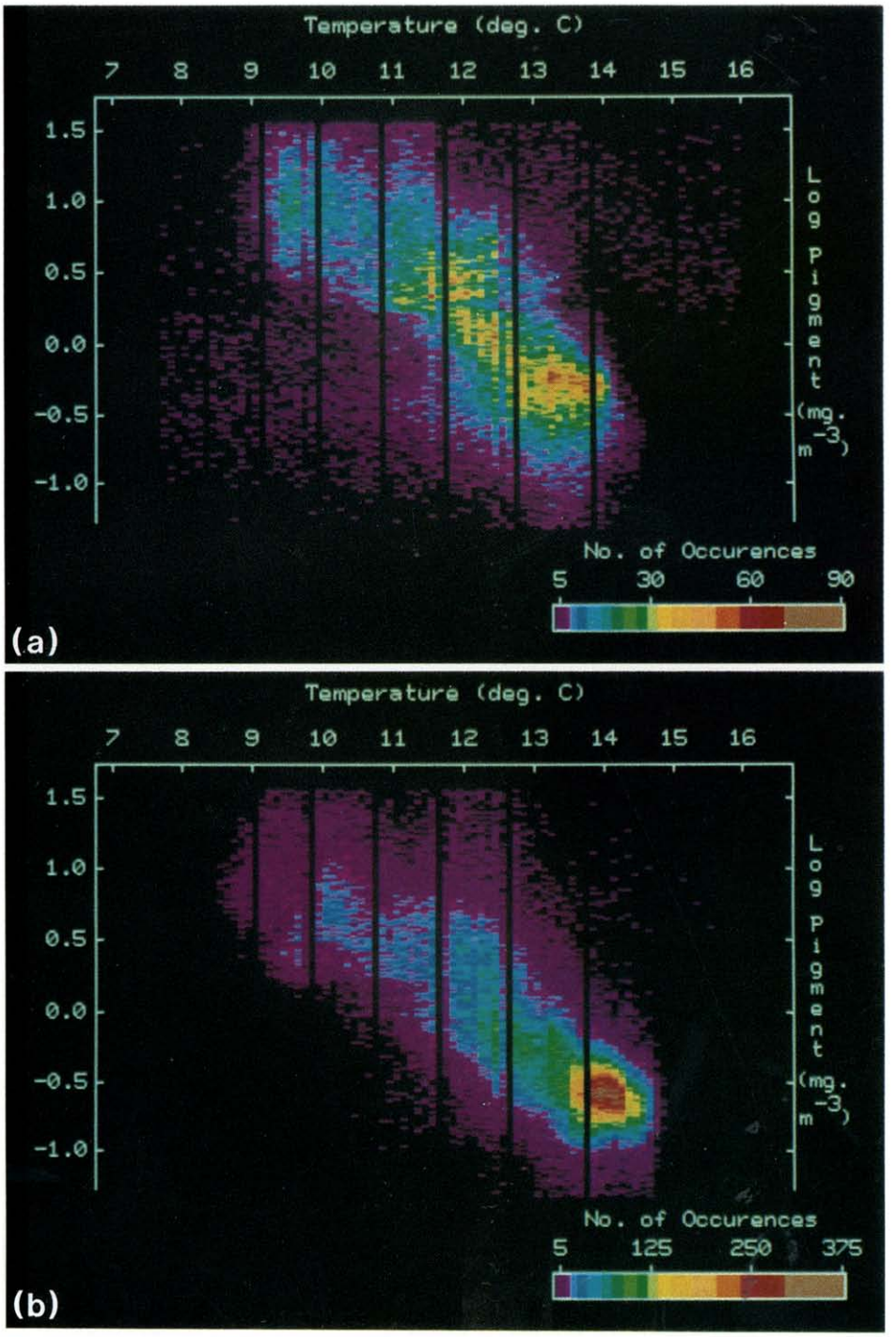

Fig. 6a and b. Caption on page 671.

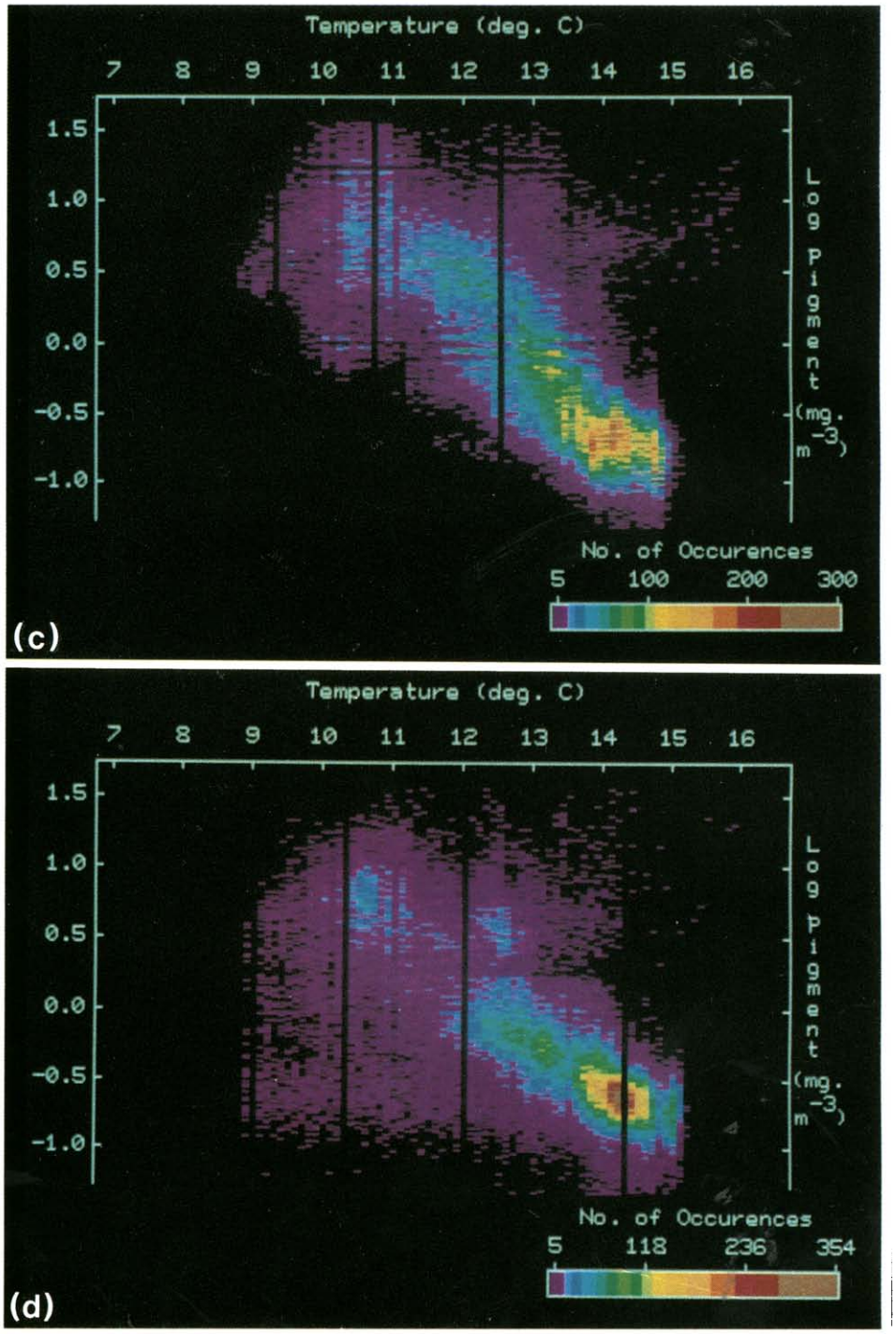
Temperature (deg. C)
7 8 9 10 11 12 13 14 15 16
1.5
1.0
0.5
0.0
-0.5
-1.0
Log Pigment (mg. m-3)
No. of Occurences
5 100 200 300
(c)
Temperature (deg. C)
7 8 9 10 11 12 13 14 15 16
1.5
1.0
0.5
0.0
-0.5
-1.0
Log Pigment (mg. m-3)
No. of Occurences
5 118 236 354
(d)

Fig. 6c and d.

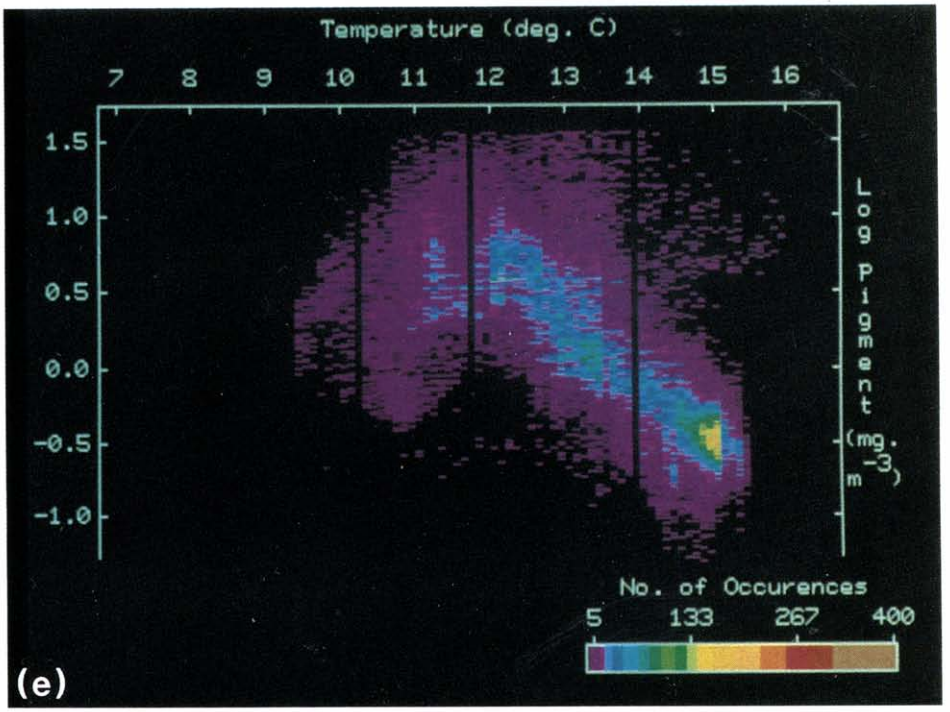

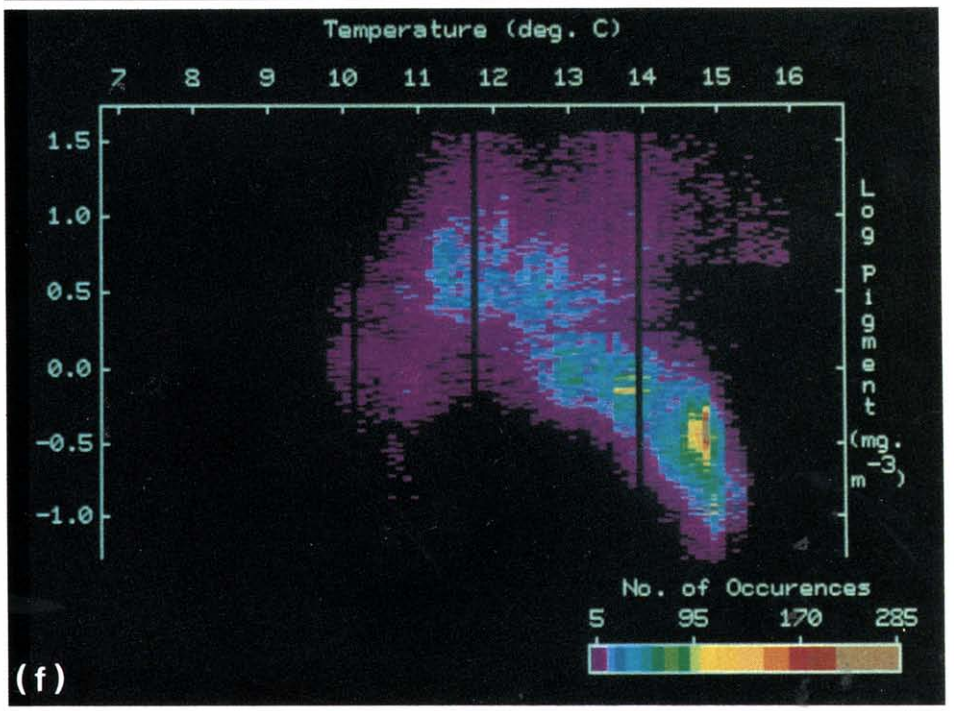

Fig. 6. (a) SST–pigment joint frequency distribution derived from AVHRR (from NOAA-6) and CZCS images from July 1981. Correlation coefficient (r) = –0.65. (b) As in (a), except from 7 July 1981. r = –0.71. (AVHRR from NOAA-6.) (c) As in (a), except from 8 July 1981. r = –0.76. (AVHRR from NOAA-7.) (d) As in (a), except from 9 July 1981. r = –0.65. (AVHRR from NOAA-7.) (e) As in (a), except from 13 July 1981. r = –0.63. (AVHRR from NOAA-7.) (f) As in (a), except from 14 July 1981. r = –0.63. (AVHRR from NOAA-7.)

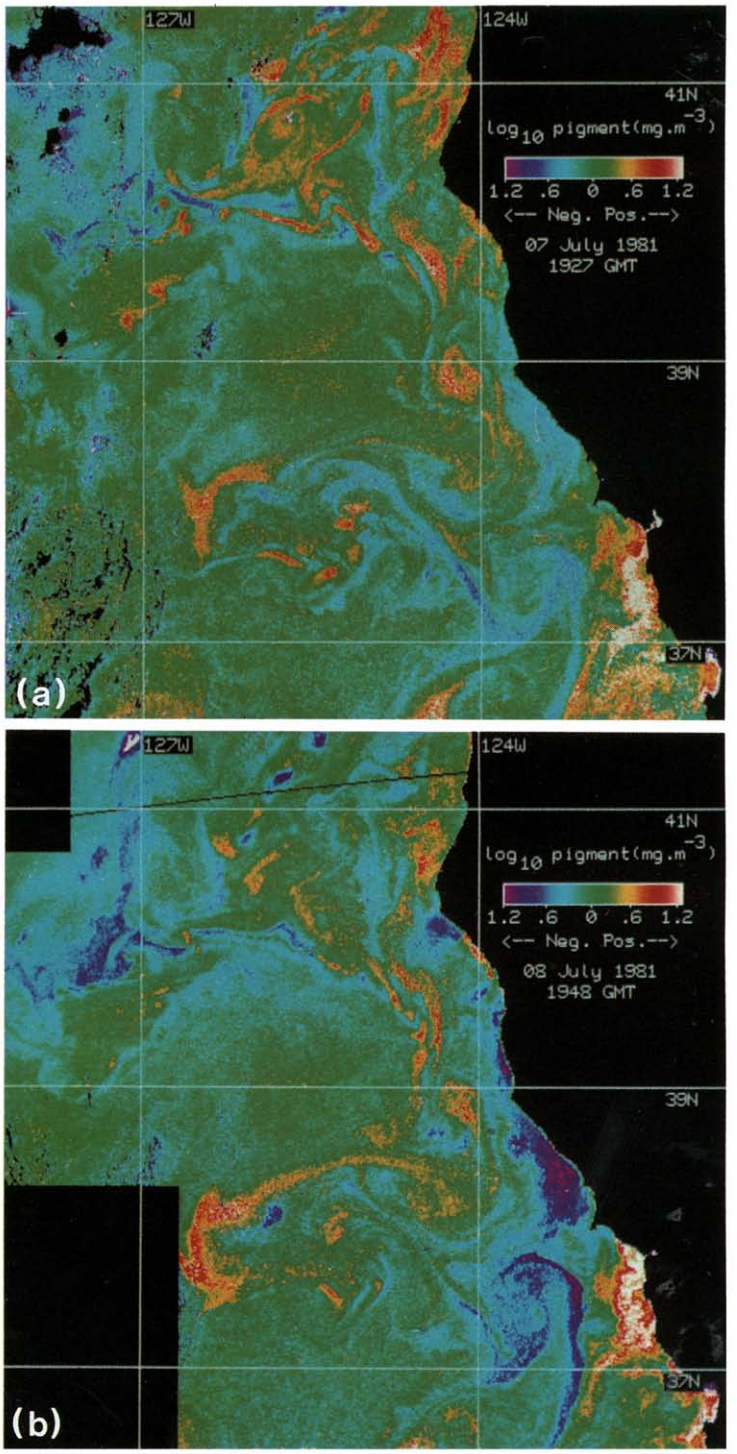
127W
124W
41N
log10 pigment(mg.m-3)
1.2 .6 0 .6 1.2
<-- Neg. Pos.-->
07 July 1981
1927 GMT
39N
37N
(a)
127W
124W
41N
log10 pigment(mg.m-3)
1.2 .6 0 .6 1.2
<-- Neg. Pos.-->
08 July 1981
1948 GMT
39N
37N
(b)

Fig. 7a and b.

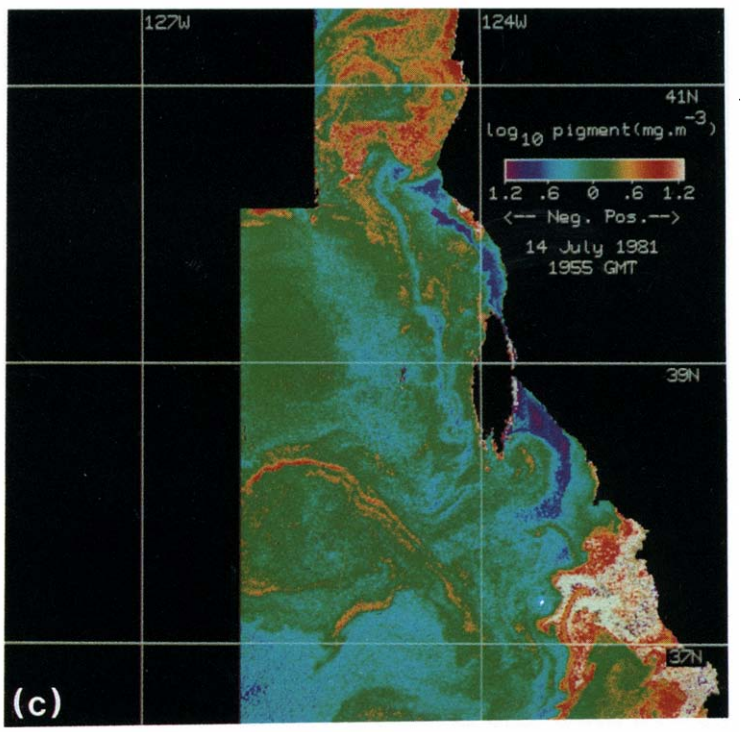

Fig. 7. (a) Difference between CZCS-estimated pigment image and SST-derived pigment image from 7 July 1981. (b) As in (a), except from 8 July 1981. (c) As in (a), except from 14 July 1981.

During the early stages of the upwelling event, the relationship between SST and pigment was relatively simple. The majority of points lay within ± 0.2 log ⟨pigment⟩ of a log-linear relationship; this result was unexpected, particularly when the degree of accuracy of the SST and pigment algorithms is considered. However, this relationship became complicated by the third day (8 July) of high winds, with the appearance of both warm, high pigment water and cold, low pigment water. The fully developed SST–pigment relationship (Fig. 6f) is characteristic of the relationships derived from ship measurements (Fig. 5). This result implies that ship-derived SST–pigment surfaces are hindered by the relatively rapid development of the SST–pigment relationship compared to the sampling time. JONES *et al.* (1983) described one instance where they noted the association of the lowest SST with the highest pigment concentrations, as during the initial stages of the July 1981 CODE upwelling event. However, the repeated, synoptic coverage by the satellite images provided a more complete view of the rapidly evolving SST–pigment relationship for a large upwelling area.

While the SST–pigment surfaces give useful information on temporal changes, they do not give any spatial information on the variability of the SST–pigment relationship. We fitted by eye a simple set of line segments through each of these six surfaces. (We chose not to use standard curve-fitting techniques as we wished to see the deviation of actual pigment concentrations from a simple, linear SST–log ⟨pigment⟩ relationship.) These day-specific curves were used as transformations to convert SST into pigment concentration, and we then formed images of the difference between actual pigment concentrations and SST-derived pigment concentrations. Such images should reveal any coherent regions that deviated from the predominant SST–pigment relationship. These difference images were used to investigate spatial variability, as well as how these spatial patterns varied over time.

Figure 7 shows three such difference images from 7, 8, and 14 July. Negative differences coincide with areas of anomalously low pigment concentration for a given temperature, and positive differences coincide with areas of anomalously high pigment concentration for a given temperature. Negative anomalies were present in nearshore waters south of Pt. Arena and Cape Mendocino and at the western end of the plume off Cape Mendocino at the beginning of the upwelling episode (Fig. 7a). Positive anomalies were present nearshore off Cape Mendocino, nearshore south of Pt. Reyes, at the offshore end of the Pt. Arena plume, and in the cold core eddy off Pt. Arena. These patterns persisted through 9 July (not shown) although the magnitudes changed somewhat. In particular, the areas of negative anomalies adjacent to Pt. Arena and Cape Mendocino had increased in size and magnitude on 8 July compared to 7 July. By 14 July (Fig. 7c), these areas had decreased in size. Also, the areas of positive anomalies near Cape Mendocino and south of Pt. Reyes had increased in extent and magnitude. The edges of the Pt. Arena plume were associated with positive anomalies throughout the upwelling event.

The upwelling zone was apparent between Cape Mendocino and Pt. Reyes as an area of anomalously low pigment concentration for a given SST. This zone was within 50 km of the coast (neglecting the offshore plumes) and reached its maximum areal extent on 8 July. Within the upwelling zone, there were several upwelling centers characterized by large negative anomalies (Fig. 7b). These centers were south of Cape Mendocino, north of Pt. Arena, and south of Pt. Arena. Analysis of the surface drifter tracks also revealed an upwelling center near Pt. Arena (DAVIS, 1985b). As with the areal extent of the upwelling zone, the upwelling centers were most pronounced on 8 July. As the winds decreased during this episode, the upwelling zone decreased noticeably in size in the offshore direction (50 km on 8 July vs 25 km on 14 July). This size reduction coincided with the reduction of upwelling at Pt.

Arena itself. The upwelling center north of Pt. Arena apparently propagated northward after 9 July. This reduction of upwelling at Pt. Arena may be associated with reduced winds; note the persistence of low morning fog at Pt. Arena on 14 July.

Just offshore of the negative anomaly region of the upwelling zone, there was a narrow (20 km) longshore band of positive anomaly water. This was apparently one of the areas where the high nutrient, upwelled water fostered intensive phytoplankton growth. There was no relation between the offshore position of this band and the edge of the shelf.

There were extensive areas of strong positive anomalies at the northern and southern ends of the upwelling zone. These regions retreated as the upwelling event began (6 to 8 July) and then moved back towards Pt. Arena as the wind stress relaxed (9 to 14 July). In particular, a positive anomaly area extended just north of Pt. Reyes on 6 July, was displaced southward by negative anomaly water by 8 July, and began to reappear north of Pt. Reyes by 14 July. The north–south expansion of the upwelling zone is consistent with the results of KELLY (1983) who showed similar expansions and contractions as a function of wind speed. The apparent nearshore northward flow near Pt. Reyes is consistent with drifter trajectories during a similar wind relaxation event in 1982 (DAVIS, 1985a).

We can speculate as to the origins of this positive anomaly water (which corresponds to high temperature, high biomass), with more confidence for the region south of Pt. Reyes where there were more *in situ* measurements. Surface measurements from previous years indicate that this region often has high chlorophyll concentrations, sometimes exceeding 30 mg m^{-3} (SIMPSON, 1985; D. CLARK, personal communication). The large upwelling zone between Cape Mendocino and Pt. Reyes probably supplies adequate nutrients to support rapid phytoplankton growth in this region. CTD surveys (OLIVERA, 1982; OLIVERA *et al.*, 1982) suggested that these waters were upwelled but had experienced local heating. Although outflow from San Francisco Bay may have an effect, it is probably relatively limited. One possible cause for these warmer waters is the reduced wind stress south of Pt. Reyes (OLIVERA, 1982; KELLY, 1983), allowing the surface waters to warm. Less wind-induced vertical mixing would allow more phytoplankton growth, because the phytoplankton would spend more time in the well-lit (and nutrient-rich) surface waters. Such increased phytoplankton biomass would increase the diffuse attentuation coefficient (AUSTIN and PETZOLD, 1981). As the diffuse attenuation coefficient is nearly a linear function of chlorophyll concentration (AUSTIN and PETZOLD, 1981), the nearly two orders of magnitude higher pigment concentration south of Pt. Reyes vs north of Pt. Reyes should have a significant effect on near-surface heating (DENMAN, 1973) as more radiation would be absorbed near the water surface. This heating would further increase the stability of the water column. In fact, both SST and pigment concentration increased in this area during this upwelling episode, relative to other areas in the images (Figs 3 and 4). Although there were no corroborative ship data, similar processes of decreased wind, increased phytoplankton growth, and increased near-surface heating may have been occurring north of Cape Mendocino. The satellite images (Fig. 3) showed a significant increase in SST during this period relative to other areas. Thus, this may be a case where biological processes (phytoplankton growth) reinforce physical processes (reduced wind mixing) and affect the physical structure of the water column (increased SST). These processes may be occurring elsewhere in this region (e.g., the small nearshore area just south of the Cape Mendocino upwelling center), but are most evident near Cape Mendocino and south of Pt. Reyes. As wind stress (hence upwelling) decreases, the supply of nutrients to these areas should also decrease, resulting in reduced phytoplankton growth. These areas then, should have decreasing SST and pigment concentrations between

upwelling events. Further investigations into the coupling of biological and physical processes in mixed layer dynamics is warranted (SIMPSON and DICKEY, 1982).

The classic zone of nearshore upwelling was interrupted by large, offshore plumes that often extended 200 to 300 km. Though the mechanisms for their formation are not clear (WILLMOTT, 1984; IKEDA and EMERY, 1984), they are associated with high offshore velocities and are relatively persistent (DAVIS, 1985a, b; KELLY, 1983; MOOERS and ROBINSON, 1984; RIENECKER *et al.*, 1985). In the difference images (Fig. 7) the plume off Cape Mendocino had a large positive anomaly area about 100 km offshore; farther offshore (200 km) there was a large negative area. The plume off Pt. Arena appeared to be the reverse, with the area of negative anomalies being inshore. This negative anomaly area appeared to be an extension of the Pt. Arena upwelling center. The intense positive area at the end of this plume (relatively high pigment concentrations for a given SST) may have been a region of exchange between the warm, nutrient-poor oceanic waters and the cool, nutrient-rich coastal waters. The Cape Mendocino plume (which appeared to originate to the north at Cape Blanco at 42.83°N, 124.53°W) appeared to move downcoast before moving offshore just north of Cape Mendocino (perhaps influenced by the Mendocino Escarpment; WILLMOTT, 1984). IKEDA and EMERY (1984) suggest that plumes south of Cape Mendocino should behave differently than those to the north as a result of different coastal topography. Note that the area of positive anomalies within this plume appeared closer to shore. In addition, the less vigorous wind mixing in this area discussed earlier may allow more active phytoplankton growth, stripping the cold upwelled water of nutrients before it is advected far offshore in the plume.

Within the Pt. Arena plume, we can estimate net phytoplankton growth rates using the pigment images and the surface drifter velocities (DAVIS, 1983). We assume that low pigment water is brought near the surface in the upwelling center and then advected offshore in the plume. Phytoplankton will begin to grow rapidly upon being exposed to higher light in this nutrient-rich water. By using the drifter velocities, we can estimate the time it took for a particular parcel to reach an offshore location away from the upwelling center. Thus, we can use a single pigment image, calculate pigment concentrations in several small areas within the plume, and use this and the derived travel time information from the drifter data to derive the growth rates. We can make these calculations after the upwelling center-plume has become fully developed. Table 1 shows the pigment values in these boxes for five of the pigment images. Note that on 6 July, pigment values were higher nearshore than offshore. By 8 July, the upwelling center was fully developed, and pigment values were lower nearshore. This pattern persisted through 14 July. On 8 July, the time for a parcel to travel from box 1 to box 5 (a distance of 70 km) was about 1.6 days. This leads to an estimated growth rate of 0.8 day^{-1}, certainly a reasonable value compared to other upwelling systems (BRINK *et al.*, 1981).

Table 1. *Mean near-surface pigment concentrations* (mg m^{-3}) *in six boxes* (410 km^2) *centered around the given location. Boxes are all within the offshore squirt near Pt. Arena*

Box	Center	6 July	7 July	8 July	13 July	14 July
1	123.31W, 38.38N	7.38	2.44	0.86	0.83	0.83
2	123.37W, 38.15N	5.75	2.81	1.57	1.75	1.71
3	123.49W, 38.00N	7.18	2.65	2.31	2.19	1.61
4	123.68W, 37.96N	4.37	2.88	2.65	2.96	2.01
5	123.87W, 37.92N	2.58	2.38	3.13	2.73	2.88
6	124.07W, 37.88N	2.88	1.66	3.13	2.96	3.31

CONCLUSIONS

The upwelling system in the CODE area appeared to be more complex than some upwelling systems (DAVIS, 1985b). In particular, the importance of spatial and temporal variability of both wind forcing and the resulting ocean circulation was important. The various CODE data sets, including the satellite images, show that the simple, linear view of coastal upwelling is too restrictive (DAVIS, 1985b). For example, there were persistent areas of preferred offshore transport, features that propagated counter to the strong downcoast winds, areas that seemed to be protected from these winds, and energetic rotating eddies. The variability of these physical processes was in large part responsible for the distribution of phytoplankton biomass. However, the relationship of these processes as expressed by SST and near-surface pigment concentration was not simple; rather it varied in both time and space.

Upwelling took place primarily within a 50 km wide band between Cape Mendocino and Pt. Reyes, which was wider than expected from linear, Ekman upwelling (GILL and CLARKE, 1974). The width of this band also depended on the wind stress. Within this band there were several upwelling centers associated with features in the coastline topography, characterized by anomalously low SST, low pigment water. The spin-up time for their development was about 2 days, after the onset of the strong downcoast winds.

The southern Pt. Arena upwelling center was associated with a large, offshore plume which advected this newly upwelled water nearly 200 km offshore. Exchange between this and nutrient-poor oceanic water seemed to occur at the offshore end of this plume. Estimates of phytoplankton growth rates using CZCS and drifter data were about 0.8 day^{-1} in this plume. A plume was present at Cape Mendocino (as well as at Pt. Sur and Pt. Conception) although this plume traveled downcoast from its origin at Cape Blanco before moving sharply offshore at Cape Mendocino.

This upwelling region was bounded on both the north and south ends by warmer, higher pigment water. Both SST and pigment concentrations increased as the winds decreased during the upwelling episode, and the warm, high pigment water began to encroach into the upwelling zone. The supply of nutrients from the upwelling areas stimulated phytoplankton growth in these less vigorously mixed areas, further increasing heating (and hence stability) of the near-surface waters.

These results show that the fortuitous coincidence of a ship survey, drifter releases, strong winds, and excellent satellite viewing conditions can lead to a more complete view of the spatial and temporal variability of biological and physical processes during upwelling. Simple analyses of the satellite data sets revealed phenomena that are worth additional study, such as the areas of high SST, high pigment concentration. Similar analyses of satellite time series from CODE and other upwelling areas could result in more realistic time and length scales required as input to numerical models (BENNETT and DENMAN, 1985). Further research on biological processes in the coastal ocean will require an increased understanding of the variability in the physical processes.

Acknowledgements—We are grateful to Drs K. A. Kelly, R. E. Davis, R. C. Beardsley, G. Holloway, and K. L. Denman for useful advice on various aspects of this work. We thank Dr. O. B. Brown, Dr. R. H. Evans, Dr. J. W. Brown, and Mr. Angel Li of the Rosenstiel School of Marine and Atmospheric Science, University of Miami, for invaluable advice and assistance with satellite data processing. Mr. F. D. Kuykendall and Mr. B. A. Houghton of JPL also provided assistance. The Scripps Satellite Oceanography Facility is supported by the National Aeronautics and Space Administration (U.S.), the Office of Naval Research (U.S.), and the National Science Foundation (U.S.). This work was carried out at the Jet Propulsion Laboratory, California Institute of Technology, under contract with NASA. This is CODE Contribution No. 11.

REFERENCES

ABBOTT M. R. and P. M. ZION (1984) Coastal Zone Color Scanner (CZCS) imagery of near-surface phytoplankton pigment concentrations from the first Coastal Ocean Dynamics Experiment (CODE-1), March–July 1981. Jet Propulsion Laboratory Publication 84-42.

AUSTIN R. W. and T. J. PETZOLD (1981) The determination of the diffuse attenuation coefficient of sea water using the Coastal Zone Color Scanner. In: *Oceanography from space*, J. F. R. GOWER, editor, Plenum Press, New York, pp. 239–256.

BEERS J. R., M. R. STEVENSON, R. W. EPPLEY and E. R. BROOKS (1971) Plankton populations and upwelling off the coast of Peru, June 1969. *Fishery Bulletin*, **69**, 859–876.

BENNETT A. F. and K. L. DENMAN (1985) Phytoplankton patchiness: inferences from particle statistics. *Journal of Marine Research* (in press).

BERNSTEIN R. L. (1982) Sea surface temperature estimation using the NOAA 6 satellite Advanced Very High Resolution Radiometer. *Journal of Geophysical Research*, **87**, 9455–9465.

BERNSTEIN R. L., L. C. BREAKER and R. WHRITNER (1977) California Current eddy formation: ship, air, and satellite results. *Science, Wash.*, **195**, 353–359.

BOJE R. and M. TOMCZAK, editors (1978) *Upwelling ecosystems*, Plenum Press, New York, 303 pp.

BREAKER L. C. and R. P. GILLIAND (1981) A satellite sequence on upwelling along the California coast. In: *Coastal upwelling*, F. A. RICHARDS, editor, American Geophysical Union, Washington, D.C., pp. 87–94.

BRINK K. H., B. H. JONES, J. C. VAN LEER, C. N. K. MOOERS, D. W. STUART, M. R. STEVENSON, R. C. DUGDALE and G. W. HEBURN (1981) Physical and biological structure and variability in an upwelling center off Peru near 15°S during March 1977. In: *Coastal upwelling*, F. A. RICHARDS, editor, American Geophysical Union, Washington, D.C., pp. 473–495.

CODE GROUP (1983) Coastal ocean dynamics. *EOS*, **64**, 538–539.

DAVIS R. E. (1983) Current-following drifters in CODE. Scripps Institution of Oceanography Reference 83–4.

DAVIS R. E. (1985a) Drifter observations of coastal surface currents during CODE: the descriptive view. *Journal of Geophysical Research* (in press).

DAVIS R. E. (1985b) Drifter observations of coastal surface currents during CODE: the statistical and dynamical views. *Journal of Geophysical Research* (in press).

DENMAN K. L. (1973) A time-dependent model of the upper ocean. *Journal of Physical Oceanography*, **3**, 173–184.

DENMAN K. L. (1983) Predictability of the marine plankton ecosystem. In: *The predictability of fluid motions*, G. HOLLOWAY and B. J. WEST, editors, American Institute of Physics, New York, pp. 601–602.

GILL A. E. and A. J. CLARKE (1974) Wind induced upwelling, coastal currents, and sea level changes. *Deep-Sea Research*, **21**, 325–345.

GORDON H. R., D. K. CLARK, J. W. BROWN, O. B. BROWN, R. H. EVANS and W. W. BROENKOW (1983a) Phytoplankton pigment concentrations in the Middle Atlantic Bight: comparison between ship determinations and Coastal Zone Color Scanner estimates. *Applied Optics*, **22**, 20–36.

GORDON H. R., J. W. BROWN, O. B. BROWN, R. H. EVANS and D. K. CLARK (1983b) Nimbus 7 CZCS: reduction of its radiometric sensitivity with time. *Applied Optics*, **22**, 3929–3931.

HICKEY B. M. (1979) The California Current System—hypotheses and facts. *Progress in Oceanography*, **8**, 191–279.

HOVIS W. A. (1981) The Nimbus-7 Coastal Zone Color Scanner (CZCS) program. In: *Oceanography from space*, J. F. R. GOWER, editor, Plenum Press, New York, pp. 213–225.

IKEDA M. and W. J. EMERY (1984) Satellite observations and modeling of meanders in the California Current System off Oregon and northern California. *Journal of Physical Oceanography*, **14**, 1434–1450.

JONES B. H., K. H. BRINK, R. C. DUGDALE, D. W. STUART, J. C. VAN LEER, D. BLASCO and J. C. KELLY (1983) Observations of a persistent upwelling center off Point Conception, California. In: *Coastal upwelling: its sediment record. Responses of the sedimentary regime to present coastal upwelling*, E. SUESS and J. THIEDE, editors, Plenum Press, New York, pp. 37–60.

KELLY K. A. (1982) Infrared satellite data from the first Coastal Ocean Dynamics Experiment: March–July 1981. Scripps Institution of Oceanography Reference 82–15.

KELLY K. A. (1983) Swirls and plumes or application of statistical methods to satellite-derived sea surface temperatures. PhD Thesis, Scripps Institution of Oceanography, 210 pp.

LEWIS M. R., J. J. CULLEN and T. PLATT (1983) Phytoplankton and thermal structure in the upper ocean: consequences of nonuniformity in chlorophyll profile. *Journal of Geophysical Research*, **88**, 2565–2570.

MCCLAIN E. P., W. G. PICHEL, C. C. WALTON, Z. AHMAD and J. SUTTON (1983) Multi-channel improvements of satellite-derived global sea surface temperatures. *Advances in Space Research*, **2**, 43–47.

MILLOT C. and L. WALD (1981) Upwelling in the Gulf of Lions. In: *Coastal upwelling*, F. A. RICHARDS, editor, American Geophysical Union, Washington, D.C., pp. 160–166.

MOOERS C. N. K. and A. R. ROBINSON (1984) Turbulent jets and eddies in the California Current and inferred cross-shore transports. *Science, Wash.*, **223**, 51–53.

NELSON C. S. (1977) Wind stress and wind stress curl over the California Current. NOAA Technical Report NMFS-SSRF-714.

OLIVERA R. M. (1982) A complex distribution of water masses and related circulation off northern California in July 1981. Master's Thesis, Oregon State University, 53 pp.

OLIVERA R. M., W. E. GILBERT, J. FLEISCHBEIN, A. HUYER and R. SCHRAMM (1982) Hydrographic data from the first Coastal Ocean Dynamics Experiment: R/V *Wecoma*, Leg 7, 1–14 July 1981. Oregon State University Reference 82-8.

RIENECKER M. M., C. N. K. MOOERS, D. E. HAGAN and A. R. ROBINSON (1985) A cool anomaly off northern California: an investigation using IR imagery and *in situ* data. *Journal of Geophysical Research* (in press).

RICHARDS F. A., editor (1981) *Coastal upwelling*, American Geophysical Union, Washington, D.C., 529 pp.

ROSENFELD L. K., editor (1983) *CODE-1: moored array and large-scale data report.* Woods Hole Oceanographic Institution Technical Report 82-23.

SCHWALB A. (1978) The TIROS-N/NOAA A-G Satellite Series. NOAA Technical Memorandum NESS 95.

SIMPSON J. J. (1985) Analytical and analysis methods for continuous underway chemical oceanographic data with application to the air–sea exchange of CO_2 and O_2. *Advances in Chemistry* (in press).

SIMPSON J. J. and T. D. DICKEY (1982) The relationship between downward irradiance and upper ocean structure. *Journal of Physical Oceanography*, **11**, 309–323.

WILLMOTT A. J. (1984) Forced double Kelvin waves in a stratified ocean. *Journal of Marine Research*, **42**, 319–358.

ZION P. M. (1983) Description of algorithms for processing Coastal Zone Color Scanner (CZCS) data. Jet Propulsion Laboratory Publication 83-98.